Soil Biology and Biochemistry 165 (2022) 108530

Contents lists available at ScienceDirect

Soil Biology and Biochemistry

journal homepage: www.elsevier.com/locate/soilbio

Plant-microbial linkages underpin carbon sequestration in contrasting mountain tundra vegetation types

Konstantin Gavazov [a,b,*], Alberto Canarini [c], Vincent E.J. Jassey [d], Robert Mills [e], Andreas Richter [c], Maja K. Sundqvist [f], Maria Väisänen [g,h], Tom W.N. Walker [i,j], David A. Wardle [k], Ellen Dorrepaal [b]

[a] Swiss Federal Institute for Forest, Snow and Landscape Research WSL, 1015, Lausanne, Switzerland
[b] Climate Impacts Research Centre, Department of Ecology and Environmental Sciences, Umeå Universitet, 98107, Abisko, Sweden
[c] Centre for Microbiology and Environmental Systems Science, Division of Terrestrial Ecosystem Research, University of Vienna, 1090, Vienna, Austria
[d] ECOLAB, Laboratoire D'Ecologie Fonctionnelle et Environnement, Université de Toulouse, CNRS, Toulouse, France
[e] Department of Environment and Geography, University of York, YO10 5DD, York, United Kingdom
[f] Department of Forest Ecology and Management, Swedish University of Agricultural Sciences, 901 83, Umeå, Sweden
[g] Ecology and Genetics Research Unit, University of Oulu, 90014, Oulu, Finland
[h] Arctic Centre, University of Lapland, 96101, Rovaniemi, Finland
[i] Department of Environmental Systems Science, ETH Zürich, 8092, Zürich, Switzerland
[j] Institute of Biology, University of Neuchâtel, 2000, Neuchâtel, Switzerland
[k] Asian School of the Environment, Nanyang Technological University, 639798, Singapore

ARTICLE INFO

Keywords:
Elevation gradient
Primary productivity
Above- and belowground interactions
C:N stoichiometry
Microbial physiology
Carbon use efficiency

ABSTRACT

Tundra ecosystems hold large stocks of soil organic matter (SOM), likely due to low temperatures limiting rates of microbial SOM decomposition more than those of SOM accumulation from plant primary productivity and microbial necromass inputs. Here we test the hypotheses that distinct tundra vegetation types and their carbon supply to characteristic rhizosphere microbes determine SOM cycling independent of temperature. In the subarctic Scandes, we used a three-way factorial design with paired heath and meadow vegetation at each of two elevations, and with each combination of vegetation type and elevation subjected during one growing season to either ambient light (i.e., ambient plant productivity), or 95% shading (i.e., reduced plant productivity). We assessed potential above- and belowground ecosystem linkages by uni- and multivariate analyses of variance, and structural equation modelling. We observed direct coupling between tundra vegetation type and microbial community composition and function, which underpinned the ecosystem's potential for SOM storage. Greater primary productivity at low elevation and ambient light supported higher microbial biomass and nitrogen immobilisation, with lower microbial mass-specific enzymatic activity and SOM humification. Congruently, larger SOM at lower elevation and in heath sustained fungal-dominated microbial communities, which were less substrate-limited, and invested less into enzymatic SOM mineralisation, owing to a greater carbon-use efficiency (CUE). Our results highlight the importance of tundra plant community characteristics (i.e., productivity and vegetation type), via their effects on soil microbial community size, structure and physiology, as essential drivers of SOM turnover. The here documented concerted patterns in above- and belowground ecosystem functioning is strongly supportive of using plant community characteristics as surrogates for assessing tundra carbon storage potential and its evolution under climate and vegetation changes.

1. Introduction

Tundra ecosystems are characterised by low-stature slow-growing vegetation, shaped by the prevailing harsh environmental conditions. Their soils are primarily composed of labile, poorly protected organic matter residues, which steadily accumulate over time as cold temperatures limit ecosystem decomposition rates more than primary productivity (Hagedorn et al., 2010; Hobbie et al., 2000). Due to the slow

* Corresponding author. Institut Fédéral de Recherches, WSL c/o EPFL-ENAC-PERL, Station 2 1015, Lausanne Switzerland.
E-mail address: konstantin.gavazov@wsl.ch (K. Gavazov).

https://doi.org/10.1016/j.soilbio.2021.108530
Received 17 October 2021; Received in revised form 16 December 2021; Accepted 18 December 2021
Available online 25 December 2021

decomposition rates, plant-available nutrients remain locked away within the soil organic matter (SOM), rendering tundra ecosystem highly nitrogen (N) limited (Hagedorn et al., 2019; Templer et al., 2012). Yet, vascular plants exhibit a range of life strategies to cope with such resource limitations (Bergmann et al., 2020), investing photosynthate into exploitative SOM-degradation pathways via mutualisms (Frey, 2019; Zak et al., 2019), direct exudation of enzymes and organic acids (Gunina and Kuzyakov, 2015; Keiluweit et al., 2015), and by stimulatory effects on rhizosphere microbes (Fontaine et al., 2007). Indeed, contrasting tundra vegetation types (i.e., vascular or nonvascular, woody or herbaceous, deciduous or evergreen) exhibit concrete functional characteristics, which to a large extent determine their potential for nutrient acquisition, productivity, and decomposability (Dorrepaal, 2007; Wookey et al., 2009). It is thus likely that they further control ecosystem functioning in terms of carbon sequestration and responses to climate change and could thus be used as proxies to assess those. In reality, however, the complexity of above- and belowground interactions involved therein has obscured the extent to which tundra vegetation type classification (e.g., Walker et al., 2005) can be scaled to the ecosystem level, due to underlying differences in environmental conditions or lack of detailed mechanistic understanding of linkages between ecosystem components.

Tundra plant community types occupy characteristic (a)biotic environments, where the supply of and demand for C and N resources in the rhizosphere results in the formation of SOM (Hagedorn et al., 2019). In general, herbaceous communities typically associate with a bacteria-dominated rhizobiome, which promotes rapid SOM turnover and high nutrient availability, while heath communities associate with a fungi-dominated rhizobiome, which favours a slow SOM cycling and low nutrient availability (Bardgett et al., 2005; Crowther et al., 2019; Wardle et al., 2004). Essentially, the characteristically high biomass C:N ratio (Strickland and Rousk, 2010) and high carbon use efficiency (CUE) (Sinsabaugh et al., 2016) of fungal-dominated communities makes these systems more conservative in their resource use. Furthermore, in contrast to meadow vegetation, taller and denser mats of heath vegetation can also cool the soil microclimate (Myers-Smith and Hik, 2013), reduce the decomposability of aboveground litter inputs (Cornelissen et al., 2007) and thereby further stimulate the accumulation of particulate SOM (Saenger et al., 2015; Väisänen et al., 2015; Vancampenhout et al., 2009). Together, these factors are likely to contribute to a higher inertia of heath than meadow tundra ecosystems to climate change.

Higher temperatures can elicit numerous direct and indirect responses in the tundra plant and soil microbial communities that regulate ecosystem C and N dynamics. On the one hand, a warmer climate stimulates tundra above- (Bjorkman et al., 2018; Väisänen et al., 2014; Yu et al., 2017) and belowground (Blume-Werry et al., 2018; Solly et al., 2017; Wang et al., 2016) plant productivity and thus increases ecosystem C inputs, provided that N availability is not limiting. This higher supply of fresh C belowground could support a larger microbial biomass and greater turnover rates, thus increasing the incorporation of microbial necromass, which represents a major source of stable soil C (Clemmensen et al., 2013, 2021; Liang et al., 2017). On the other hand, warmer climate also stimulates soil microbial physiology (Walker et al., 2018; Xue et al., 2016) and thereby the mineralisation of the large SOM stocks, potentially increasing N availability (Karhu et al., 2014; Mack et al., 2004). The microbial synthesis of costly extracellular enzymes, which degrade SOM, can further be stimulated through enhanced plant productivity and the exudation of labile photosynthates in the rhizosphere of certain, albeit not tundra, woody vegetation (Clemmensen et al., 2021; Hartley et al., 2012; Parker et al., 2015). It remains thus questionable whether primary productivity of functionally different tundra vegetation types consistently enhances nutrient availability in the rhizosphere, through accelerated mineralisation of tundra soil organic stocks, and to what extent temperature modulates this process.

Aiming to bridge this knowledge gap, here we installed an experiment along an elevation gradient on Mt Suorooaivi in subarctic Sweden (Sundqvist et al., 2011) to explore how the effects of belowground plant photosynthetic input on mountain tundra C and N cycling vary with elevation within two dominant tundra vegetation types. We focused on two elevations above the treeline as proxies for long-term ecosystem adaptations to different climate regimes (Elmendorf et al., 2015; Körner, 2007). At both elevations, heath and meadow communities grow in mosaic patterns and thus allow direct comparisons, independent of environmental conditions (Fig. 1a–b). Within each elevation × vegetation combination, we established a shading treatment during one growing season (Fig. 1c), in order to temporarily limit plant productivity and thus the seasonal input of C belowground, in comparison to ambient conditions (Bahn et al., 2013; Kuzyakov, 2006; Möhl et al., 2019; Rinnan et al., 2007).

In this study system we sought to test three hypotheses. First, we hypothesised that, in comparison to meadow vegetation, heath vegetation would have a more fungal-dominated community, with higher stoichiometric plasticity and higher CUE, and that these associate with lower SOM turnover rates (e.g., substrate uptake and respiration, extracellular enzymatic activity, ecosystem respiration). This difference between vegetation types would be independent of elevation (i.e., the long-term difference in climate regimes). Second, we hypothesised that, due to warmer temperatures, both vegetation types at the low elevation site would have higher rates of plant and microbial physiological processes, as well as C and N biogeochemical cycles that associate with more bacteria-dominated communities. This effect is expected to be stronger at the meadow than at the heath, due to higher vegetation buffering of microclimate under heath systems. Third, we hypothesised that the photosynthate supply belowground would represent a major C and energy source for tundra microbial communities and thus determine their biomass, growth and turnover, and, ultimately, the ecosystem potential for C sequestration. We expected that, due to this pivotal plant role, these effects would be independent of elevation and vegetation type. In assessing these three hypotheses in combination, we contribute to a comprehensive understanding of the interlinked above- and belowground mechanisms for C cycling in tundra ecosystems.

2. Materials and methods

2.1. Experimental design and plant productivity manipulation

The study was conducted during the 2016 plant growing season (11 July – 26 September) on the north-east slope of Mt Suorooaivi (Fig. 1a) in the Swedish subarctic (68°17′01.4″N 19°06′51.1″E). Growing season records during 2002–2011 for temperature and precipitation in the area (Abisko Scientific Research Station, 380 m asl) are 10.9 °C and 138 mm, respectively (Callaghan et al., 2013). The local treeline occurs at 500–600 m asl and is formed of mountain birch *Betula pubescens* ssp. *czerepanovii*, with vegetation above the treeline comprising a mosaic of vegetation types, including heath and meadow communities. The heath community is dominated by the ericaceous dwarf shrubs *Empetrum nigrum*, *Vaccinium uliginosum*, *V. vitis-idaea*, as well as dwarf birch, *Betula nana*. The meadow community is dominated by the graminoids *Deschampsia flexuosa* and *Anthoxanthum alpinum*, *Carex bigelowii* and the forbs *Saussurea alpina*, *Viola biflora* and *Solidago virgaurea*.

We selected 24 homogeneous patches of heath and meadow communities at two elevations (700 and 900 m asl) above the treeline and within a three km distance from each other (n = 6, Fig. 1a–b) in order to compare ecosystem functioning at two different temperature regimes. The proximity of the two sites ensured that besides the typical temperature lapse rate with elevation, the effect of other climatic factors was minimised. This corresponds to a mean growing season temperature shift of 1.5 K and no change in precipitation sums for our two elevations sites (Sundqvist et al., 2011; Veen et al., 2015). At each elevation, patches within the same vegetation type were spaced at a 5–10 m distance from each other, and those between vegetation types – at approximately 100 m. Owing to the high small-scale spatial

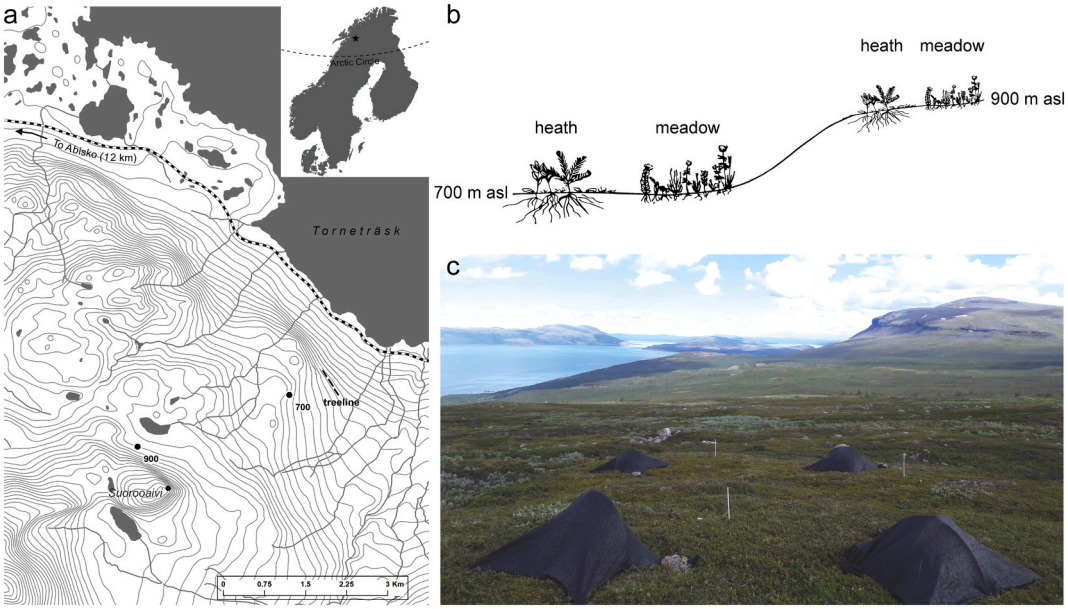

Fig. 1. Experimental setup showing (**a**) a map of the two elevations sites lying at a three km distance along the gentle (4–10°) north-east facing slope of Mt Suorooaivi and (**b**) a diagram of the target vegetation types found within 100 m distance from each other at both elevations above the natural treeline. Within each elevation and vegetation type (n = 6), we used shading tents (**c**) to reduce incoming solar radiation during the growing season (11 July – 26 September 2016) by 95% compared to adjacent paired control plots lying within 1 m away (white marking sticks) in order to discern the effects of plant productivity on microbial physiology and ecosystem C and N cycling.

heterogeneity in these communities (Björk et al., 2007), this distance is sufficient to ensure adequate independence among the patches (Sundqvist et al., 2012). Within each vegetation-elevation patch, we created two paired 0.5 × 0.5 m plots, within 1 m distance from each other. Adjacent plots in a pair were randomly assigned to either ambient or shaded light conditions (Fig. 1c). The latter was achieved using 1 × 1 × 0.5 m (L × W × H) tents made of UV-resistant mesh, which intercepts incident light, yet should not affect precipitation (Gavazov et al., 2014, see Fig. S3). The ambient vs. shaded treatment allowed us to quantify the direct effects of seasonal plant productivity (Schmitt et al., 2013; Warren et al., 2012) and root exudation (Hill et al., 2007; Zagal, 1994) on soil microbial physiology and C and N cycling, independently from elevation and vegetation type and without interfering with the vegetation structure or biomass (Table 2). To limit the influx of belowground inputs from the surrounding vegetation, all plots were delimited at the border by trenching roots and hyphae down to the bedrock (about 20 cm depth) with a serrated knife. We logged hourly soil temperature at 10 cm depth in three replicate pairs of ambient and shaded plots within each vegetation type and elevation using Tinytag thermocouples (Inlab, Sweden). In one of these pairs, air temperature and incident light was also measured hourly using Pendant HOBO loggers (Onset, USA) installed at 10 cm height above the vegetation canopy and, for the shaded treatment, underneath the shading mesh (Fig. S1).

We validated the efficiency of the shading tents in reducing plant productivity and the likely supply of photosynthates belowground by using measurements of potential atmospheric CO_2 exchange (Fig. S2). Measurements were taken in the centre of all plots during peak biomass on 4 August 2016 in optimal sunlight or within the shading tents (09:30 to 16:00) using a portable EGM4 infrared gas analyser (PP Systems, USA) equipped with a CPY-4 transparent canopy chamber (2.5 l volume). We created an airtight seal within the chamber by attaching it to a custom-made PVC collar (15 cm diameter, 5 cm height) with a plastic skirt pressed tight onto the surrounding vegetation. Following net ecosystem CO_2 exchange (NEE) measurements in each plot, the transparent chamber was flushed with ambient air, then replaced on the collar and covered with an opaque lid for measuring ecosystem respiration (ER). Each measurement lasted 1 min in order to avoid the build-up of heat and condensation inside the chamber. We calculated CO_2 fluxes as a linear change in CO_2 concentration (ppm) over the measurement period, taking into account ambient atmospheric pressure and gas temperature. Gross ecosystem productivity (GEP) was calculated as the difference between ER and NEE. These measurements showed that shading reduced the amount of incident light arriving at the vegetation canopy by approximately 95% (Figs. S1a–b), and GEP by 94% (GEP not significantly greater than zero at P = 0.220; Fig. S2a).

2.2. Plant and soil sampling

At the end of the experiment, plant aboveground biomass from a central 20 × 20 cm square in each plot was clipped at the soil surface and dried at 60 °C until constant weight was achieved (approximately 2 days). Within these bare patches, two to three soil cores were taken with a serrated steel corer (4.5 cm diameter, 10 cm depth) and homogenised to account for fine scale belowground heterogeneity (Baldrian, 2014). Subsamples were used to determine gravimetric water content by drying at 105 °C (Fig. S3) and maximum water holding capacity by saturation through capillary water rise. The remaining soils were adjusted with MilliQ to 60% of their water holding capacity and kept at 10 °C (i.e., average peak growing season temperature across all treatments) until further standardized microbial analyses (see section 2.4). Soil organic C and N concentrations were measured on ground dry soil with an elemental analyser (Carlo Erba 1110, CE Instruments).

2.3. Soil solution analyses

Soil N availability was determined using commercial resin bags (Unibest, USA) placed at the centre of each plot within the main rooting zone at 5 cm soil depth for the duration of the entire growing season (11 July – 26 September 2016). Upon collection, ammonium and nitrate were extracted from the resin bags (30 ml 1M KCl, 2 h) and analysed on a FIAstar 5000 (FOSS, Sweden). Weakly bound dissolved organic matter (DOM) in soil solution was obtained by percolating 40 ml MilliQ through a column containing a 10 g fresh weight soil subsample and allowing it to drain by gravity. The solution was then passed through 0.45 μm glass

microfiber filter to remove suspended microbial cells and analysed for dissolved organic C (DOC) and dissolved total N (DTN) on a TOC-VCPH equipped with a TNM-1 unit (Shimadzu). The extent of DOM decomposition, i.e. the humification index (HIX), was determined spectrophotometrically (Spectramax M3 Molecular Devices) as the ratio of fluorescence resulting from UV excitation at 254 nm and emission at 435–480 nm divided by the sum of emission at 300–345 nm and 435–480 nm (Ohno, 2002).

2.4. Soil microbial analyses

The affinity of soil microbes to take up and mineralise plant-derived organic substrates was quantified using a spike of uniformly-labelled 99 atom% ^{13}C glucose (Sigma-Aldrich) as a tracer. Paired 20 g fresh soil subsamples from each plot were enclosed in 300 ml glass vials with rubber septa, flushed with CO_2-free synthetic air and incubated at 10 °C for 24 h with 1 ml of either 150 μg C g^{-1} dry soil ^{13}C glucose solution (<10% of microbial biomass C), or with 1 ml of MilliQ water. Concentrations and stable isotopic signatures of CO_2 were determined on 20 ml headspace samples injected into an isotopic CO_2 spectrometer, equipped with a small sample isotope module (Picarro G2131-*i*, USA). Following corrections for gas temperature and pressure, substrate-induced respiration was calculated as the excess ^{13}C–CO_2 of enriched samples relative to corresponding natural abundance samples.

At the end of the 24 h incubation, soils were freeze-dried for phospholipid fatty acids (PLFA) analysis. Lipids were extracted from lyophilised soil subsamples with a solution of chloroform, methanol and phosphate buffer (1:2:0.8 vol), and then separated into neutral, glyco-, and phospholipids on silica solid phase extraction cartridges (Supelco, Merck, Darmstadt, Germany). The phospholipids were subsequently trans-esterified into fatty acid methyl esters using methanolic KOH. PLFA biomarkers and their respective $\delta^{13}C$ signatures were quantified on a Trace GC Ultra connected by a GC-IsoLink to a Delta V Advantage Mass Spectrometer (all Thermo Fisher Scientific) with reference to methyl nonadecanoate (19:0) as internal standard. Glucose uptake was quantified as the excess incorporation of ^{13}C into individual PLFA biomarkers in enriched samples relative to that in natural abundance samples and reported as microbial mass-specific total substrate uptake. Following standard notation, we identified PLFA biomarkers i15:0, a15:0, i16:0, i17:0, a17:0 as gram positive (G+) bacteria (Schnecker et al., 2012), biomarkers 16:1ω7, cy17:0, cy19:0 as gram negative (G-) bacteria (Kaiser et al., 2010b; Schnecker et al., 2012), biomarkers 10Me16:0, 10Me17:0 as actinobacteria (Schnecker et al., 2012; Zelles, 1999), biomarkers 14:0, 17:1ω7, 17:0 as general bacteria (Kaiser et al., 2010b; Phillips et al., 2002; Schnecker et al., 2012), biomarker 16:1ω5 as arbuscular mycorrhizal (AM) fungi (Fuchslueger et al., 2014; Olsson, 1999), biomarker 18:2ω6,9 as ectomycorrhizal (ECM) fungi (Högberg et al., 2010; Kaiser et al., 2010a; Olsson, 1999; Streit et al., 2014), biomarkers trans18:1ω9, cis18:1ω9 as general fungi (Schnecker et al., 2012), biomarker 20:4ω6,9,12,15 as protozoa (Ruess and Chamberlain, 2010) and biomarkers 16:0, 18:0, 20:0 as general PLFAs (Schnecker et al., 2012).

Microbial growth was determined by the incorporation of ^{18}O-labelled water into DNA over time in a separate incubation. Within one week from sampling, paired 0.5 g fresh soil samples were incubated at 10 °C for 24 h with either 20 atom% ^{18}O-labelled water or molecular grade water as a natural abundance control. Following the incubation, soil was snap frozen in liquid N_2 and DNA was extracted (FastDNA SPIN Kit for Soil, MP Biomedicals), quantified (Quant-iT PicoGreen dsDNA Assay Kit; Thermo Fisher) and analysed for $\delta^{18}O$ signature and O concentration on an elemental analyser coupled to a Delta V Advantage IRMS via a Conflo III (Thermo Fisher). Following Walker et al. (2018), we derived microbial community turnover as the daily mass-specific growth rates, assuming a steady state of the microbial pool size. Further, microbial respiration was determined by gas chromatography (Trace GC Ultra; Thermo Fisher) on gas samples taken at the start and end of the incubation period and used to derive carbon use efficiency (CUE) as the ratio of microbial growth versus the sum of microbial growth and respiration (Walker et al., 2018). Microbial biomass C and N concentrations were determined by the difference between paired chloroform fumigated and non-fumigated sample aliquots extracted with 1M KCl on a TOC-VCPH/CPNTNM-1 analyser, using 0.45 and 0.54 conversion factors for their respective extraction efficiencies. Microbial biomass C was further used to standardise all measures of microbial activity per unit biomass as mass-specific rates.

Extracellular enzymes (EE) were extracted within a day from sampling from 3 g fresh soil in a 50 ml extraction solution (0.1 M $CaCl_2$, 0.05% Tween 80, 20 g polyvinylpolypyrrolidone). The supernatant (centrifuged 10 min, 10 000 g, 4 °C) was filtered (1.2 μm glass microfiber) and concentrated in dialysis tubes (10–12 kDa molecular mass cut-off, Medicell Membranes Ltd) overnight at 4 °C covered with polyethylene glycol (Criquet et al., 1999; Jassey et al., 2012). Concentrated EE were re-suspended in 10 ml of phosphate buffer (1/5 of the initial volume) and split into two aliquots – one intact (5 ml) and one (5 ml) quenched control (3 h, 90 °C) to correct for background optical interferences. The potential overall hydrolytic enzyme activity was determined by a fluorescein diacetate (FDA) assay and the potential decomposition of cellulose by a β-glucosidase (BG) assay. Potential enzymatic oxidation of lignin and other aromatic compounds was determined by phenoloxidase (PO) and peroxidase (PER) assays. For hydrolytic activities, 38 μl aliquots of intact and quenched EE extracts were mixed with 250 μl of fluorogenic substrate [200 μM, fluorescein diacetate for FDA and 4-methylumbelliferyl (MUF)-β-D-glucopyranoside for BG] and incubated in microplates (3 h, 25 °C, in dark). Fluorescence was detected on a spectrophotometer (Spectramax M3 Molecular Devices) with excitation – emission wavelengths set at 490 nm–523 nm for FDA and 365 nm–450 nm for BG, and their respective activities were quantified against fluorescein and MUF standard curves. For oxidative activities, 150 μl aliquots of intact and quenched EE extract were mixed with 2 μl chromogenic substrate diaminofluorene (DAF, 0.68 mM). For PER, 10 μl 0.3% H_2O_2 were added to the reaction. Absorbance at 600 nm was measured immediately on a spectrophotometer and the kinetics were followed for 1h until saturation. All oxidative EE activities were quantified with a DAF emission coefficient 10228 M^{-1} cm^{-1}.

2.5. Statistical analysis

The experimental design comprised 48 plots distributed across two levels of the shading treatment, two vegetation types and two elevations, with six replicates for each factorial combination. The effects of these three fixed categorical factors and their two- and three-way interactions on biogeochemistry and microbial physiology were assessed by fitting linear mixed effect models, which included the 24 pre-selected vegetation patches as a random intercept term to account for pairing ambient and shaded plots within a given patch. Significance ($P < 0.05$) was determined by likelihood ratio (LR) tests between models including or excluding explanatory variables. Where necessary, we controlled for unequal variance between explanatory factor levels and log-transformed response variables to meet model assumptions. Results from all final models are presented in Table 2. We tested for effects of explanatory variables on microbial community composition (PLFA data) using non-metric dimensional scaling (NMDS) based on Bray-Curtis dissimilarity, followed by a PERMANOVA test. All analyses were performed on R version 3.5.1 (R Core Team, 2018), using the *nlme* package (Pinheiro et al., 2018) for mixed-effect models and the *vegan* package (Oksanen et al., 2019) for NMDS and PERMANOVA.

The accumulation of SOC in tundra ecosystems is controlled by temperature across elevations, vegetation composition and photosynthate inputs via numerous interconnected biotic and abiotic mechanisms that operate simultaneously. We explored such complex interactions using structural equation modelling, SEM (Grace et al., 2014). Following current knowledge of tundra above- and belowground linkages with

climate and vegetation (Hagedorn et al., 2019; Mayor et al., 2017), we developed an *a priori* conceptual model of all hypothesised relationships among the measured biogeochemical parameters within a path diagram (Fig. S4). It provides a causal interpretation of expected effects of elevation, vegetation type, and experimental shading on soil organic carbon accumulation, cascading through a network of above- and belowground linkages (Grace et al., 2014; Jassey et al., 2018; Prommer et al., 2020). Our SEM approach was semi-exploratory in that while we worked to address general hypotheses embodied in the path diagram, the precise variables used were determined empirically based on their collinearity, the outputs of the full model and by step-wise exclusion/selection of linkages among variables, as estimated by AIC (Grace et al., 2016). To that end, we used NMDS axis 1 as a proxy for microbial community composition and expressed all EE activities as a multi-functionality (MF) index based on Z-scores (Jassey et al., 2018). Here, high values of MF enzymes represent high values of many, but not necessarily all, individual enzyme activities (Jassey et al., 2018). Path analysis was performed using the *piecewiseSEM* R package (Lefcheck, 2016) using linear mixed effect models as described above.

3. Results

3.1. Above- and belowground C and N pools and fluxes

Aboveground plant biomass was 3.5 three times higher in the heath than in the meadow, independent of elevation (Table 1, Table 2). Compared to the meadow, maximum temperatures in the heath soil remained lower at a given elevation and did not change as much in response to the shading treatment (Fig. S1c). GEP estimates from the peak growing season were approximately 50% lower in the heath than in the meadow (Table 1, Fig. S2a). Further, topsoil under heath vegetation held an order of magnitude larger C and N stocks than did the topsoil under meadow vegetation, and had twice as high C:N ratio and one unit lower pH (Table 1, Table 2). The stocks, as well as their C:N ratio, were all lower at the high elevation for both vegetation types (Table 1, Table 2). These soil C and N patterns were further reflected in the soil solution C and N pools across vegetation types and elevations (Fig. 2c–e, Table 2).

The amount of plant available ammonium and nitrate in ambient plots, as integrated over the plant growing season in buried resin bags, was generally higher at the high elevation and in the meadow, despite the lower soil N stocks and water-soluble total N there (Fig. 2a–c, Table 1, Table 2). Compared to the low elevation, at the high elevation, there was more available ammonium in the heath and more nitrate in the meadow (Fig. 2a–b, Table 2). Both soil solution C:N ratio (Fig. 2e, Table 2) and its degree of humification (Fig. 2f, Table 2) at the end of the growing season were greater at the low elevation and in the heath.

The strong reduction of seasonal plant productivity caused by the shading treatment did not affect the standing aboveground biomass at the end of the growing season in either vegetation type (Table 2). Yet, it strongly increased the availability of ammonium and nitrate in the meadow during the growing season, as well as the total amount of water-soluble DTN and DOC at the end of the growing season (Fig. 2a–c, Table 2). This effect was particularly pronounced at the high elevation, where shading increased the amounts of exchangeable nitrate and DTN several fold (Fig. 2a–c, Table 2). As a result, shading caused a decrease in soil solution C:N ratio in the meadow (Fig. 2e, Table 2). In contrast, the soil solution C:N ratio was increased by shading in the heath, as the total amount of DOC increased more than did DTN (Fig. 2e, Table 2).

Table 1
Elevation and vegetation type patterns in above- and belowground (10 cm depth) organic matter stocks along the Mount Suorooaivi gradient. Presented are average (±SE) values for ambient plots (n = 6). Detailed statistical comparisons are shown in Table 2.

	700 m asl		900 m asl	
	Heath	Meadow	Heath	Meadow
Plant aboveground biomass (kg m^{-2})	0.680 ± 0.091	0.201 ± 0.055	0.607 ± 0.039	0.190 ± 0.051
Gross ecosystem productivity (g C m-2 h-1)	0.316 ± 0.045	0.531 ± 0.103	0.147 ± 0.046	0.360 ± 0.094
Soil organic carbon stock 0–10 cm (kg C m^{-2})	3.131 ± 0.286	0.757 ± 0.055	3.086 ± 0.291	0.313 ± 0.014
Soil total nitrogen stock 0–10 cm (kg N m^{-2})	0.119 ± 0.014	0.053 ± 0.004	0.135 ± 0.012	0.027 ± 0.002
Soil organic matter C:N ratio	27.1 ± 1.9	14.4 ± 0.2	23.2 ± 1.8	11.5 ± 0.2
Soil pH	4.29 ± 0.09	5.60 ± 0.10	4.54 ± 0.13	5.43 ± 0.03
Organic layer depth (cm)	5.4 ± 0.5	2.2 ± 0.2	6.2 ± 1.0	2.2 ± 0.3

3.2. Soil microbial biomass and community composition

Soil microbial biomass in ambient plots was four-fold greater in the heath than in the meadow and was larger at low elevation for both vegetation types (Fig. 3a, Table 2). Experimental shading significantly reduced microbial biomass in both vegetation types at low elevation, but not at high elevation (Fig. 3a, Table 2). Microbial biomass C:N ratio and the relative abundance of fungal to bacterial PLFA markers (F:B ratio) were larger in the heath and at low elevation (Fig. 3b–c, Table 2). Soil microbes had a narrow range of C:N ratios (between 3 and 13) and, except for the high elevation meadow, the communities were dominated by fungi (i.e., F:B ratio >1). Experimental shading reduced microbial C:N ratios consistently across both elevations and vegetation types, but did not alter the F:B ratio, nor the overall PLFA-derived microbial community composition (Fig. 3d). Microbial communities differed significantly between the vegetation types, with a clear separation along the NMDS axis 1 (Fig. 3d). The heath was dominated by PLFA-markers associated with ectomycorrhizal fungi, saprophytic fungi and protozoa, whereas the meadow by actinobacteria, gram positive bacteria and arbuscular mycorrhizal fungi. Furthermore, actinobacteria were more common at the low elevation and protozoa were more common at high elevation sites.

3.3. Soil microbial physiology

Mass-specific microbial respiration rates under meadow vegetation were two-fold higher at the high than at the low elevation, whereas under heath vegetation respiration rates did not vary with elevation and had intermediate rates compared to the two meadow elevations (Fig. 4a, Table 2). Experimental shading did not affect mass-specific microbial respiration in either vegetation type (Fig. 4a, Table 2). However, shading caused a consistent increase in microbial substrate respiration rates (i.e., mineralisation of ^{13}C-labelled glucose) at both elevations in the meadow but had no effect on these rates in the heath (Fig. 4b, Table 2). In addition, whereas heath microbes at both elevations mineralised only a small proportion of this substrate (i.e., about 10% relative to basal respiration rates), in meadows this was much greater, especially at high elevation, where substrate addition nearly doubled microbial respiration rates (i.e., about 100% relative to basal respiration rates). The incorporation of ^{13}C-labelled glucose into microbial biomass (i.e., sum of all PLFA biomarkers) was more pronounced at the high elevation for both vegetation types, and this pattern was stronger for the meadow (Fig. 4c, Table 2). Microbial CUE was not significantly affected by the shading treatment and was greater at the low elevation where it was similar between the two vegetation types (Fig. 4d, Table 2). Microbial CUE was approximately 30% less in the heath and 50% less in the meadow at the high compared to the low elevation (Fig. 4d, Table 2). The microbial biomass turnover was faster at the low elevation and in the heath than at high elevation and in the meadow (Fig. 4e, Table 2). Whereas microbial turnover rates accelerated due to the shading treatment in the heath, they decelerated in the meadow and these effects

Table 2
Likelihood ratios (LR), denominator degrees of freedom (df) and probabilities (P, in bold when significant) for statistical comparisons of the effects of vegetation type, elevation and experimental shading and their two- and three-way interactions on response variables presented in the text. *log* indicates those variables which were logarithm-transformed to meet underlying assumptions of the statistical tests.

Response	Vegetation (V)			Elevation (E)			Shading (S)			V × E interaction			V × S interaction			E × S interaction			V × E × S interaction		
	LR	df	P	LR	df	P	LR	df	P	LR	df	P	LR	df	P	LR	df	P	LR	df	P
Plant AGB stock	46.5	23	**0.000**	0.2	23	0.626	1.7	23	0.194	0.0	21	0.966	0.0	21	0.938	0.0	21	0.839	1.0	20	0.306
Topsoil OC stock	85.9	23	**0.000**	14.1	23	**0.000**	2.2	23	0.134	0.1	21	0.731	0.6	21	0.435	5.3	21	**0.021**	0.9	20	0.334
Topsoil TN stock	57.9	23	**0.000**	5.4	23	**0.020**	2.4	23	0.124	3.1	21	0.080	0.5	21	0.471	5.2	21	**0.023**	1.8	20	0.176
Topsoil C:N ratio	78.6	23	**0.000**	37.4	23	**0.000**	0.0	23	0.914	0.7	21	0.388	0.0	21	0.962	0.0	21	0.987	0.1	20	0.759
log GEP rate	6.6	22	**0.010**	6.6	22	**0.010**	30.4	22	**0.000**	1.3	20	0.257	0.5	20	0.464	3.7	20	0.056	0.3	20	0.582
ER rate	1.2	22	0.274	7.3	22	**0.007**	15.2	22	**0.000**	2.2	20	0.138	10.4	20	**0.001**	0.4	20	0.530	0.7	20	0.415
NEE rate	8.7	23	**0.003**	4.0	23	**0.046**	29.6	23	**0.000**	0.7	21	0.392	2.6	21	0.104	7.9	21	**0.005**	0.2	20	0.651
GWC	69.3	23	**0.000**	1.1	23	0.287	7.7	23	**0.006**	5.2	21	**0.022**	0.7	21	0.389	3.7	21	**0.050**	3.3	20	0.068
NH4 availability	3.2	23	0.074	4.1	23	**0.043**	8.5	23	**0.004**	4.2	21	**0.040**	10.0	21	**0.002**	0.5	21	0.504	0.1	20	0.799
log NO3 availability	20.5	23	**0.000**	2.4	23	0.123	6.2	23	**0.013**	19.2	21	**0.000**	11.1	21	**0.001**	0.0	21	0.921	0.5	20	0.505
log TN in soil solution	34.0	21	**0.000**	7.6	21	**0.006**	7.0	21	**0.008**	1.2	20	0.266	5.9	20	**0.015**	7.9	20	**0.005**	10.2	20	**0.001**
log OC in soil solution	63.7	21	**0.000**	13.2	21	**0.000**	0.1	21	0.711	0.3	20	0.564	5.3	20	**0.021**	0.5	20	0.484	0.0	20	0.959
C:N in solution	42.6	21	**0.000**	7.7	21	**0.006**	4.1	21	**0.044**	0.0	20	0.849	19.7	20	**0.000**	16.6	20	**0.000**	4.6	20	**0.032**
Humification index	52.5	23	**0.000**	22.3	23	**0.000**	18.5	23	**0.000**	3.3	21	0.071	1.1	21	0.300	0.7	21	0.406	0.7	20	0.389
Microbial biomass C	46.8	23	**0.000**	23.7	23	**0.000**	4.2	23	**0.040**	1.0	21	0.312	1.1	21	0.291	5.4	21	**0.020**	0.0	20	0.804
Microbial biomass C:N	13.6	23	**0.000**	5.1	23	**0.025**	9.1	23	**0.003**	0.2	21	0.651	0.7	21	0.403	1.1	21	0.303	2.1	20	0.151
Fungal:bacterial ratio	26.6	23	**0.000**	7.9	23	**0.005**	1.5	23	0.218	0.9	21	0.354	0.5	21	0.463	0.2	21	0.644	0.3	20	0.609
Microbial respiration	9.2	22	**0.002**	10.2	22	**0.001**	0.2	22	0.646	7.2	20	**0.007**	0.2	20	0.625	1.1	20	0.291	0.1	20	0.731
log ^{13}C respiration	26.1	11	**0.000**	4.8	11	**0.029**	0.0	11	0.834	8.0	9	**0.005**	5.7	9	**0.017**	0.5	9	0.502	0.4	8	0.533
log ^{13}C PLFA uptake	39.8	23	**0.000**	27.6	23	**0.000**	0.0	23	0.935	14.7	21	**0.000**	0.1	21	0.744	5.4	21	**0.020**	3.4	20	0.064
Carbon use efficiency	7.5	22	**0.006**	30.7	22	**0.000**	0.1	22	0.712	5.5	20	**0.019**	1.2	20	0.265	1.1	20	0.295	0.3	20	0.610
log Turnover rate	29.1	23	**0.000**	25.7	23	**0.000**	0.7	23	0.413	0.7	21	0.401	12.8	21	**0.000**	4.3	21	**0.038**	0.1	20	0.760
Fluorescein diacetate	1.0	23	0.328	0.5	23	0.491	4.8	23	**0.029**	1.9	21	0.171	0.8	21	0.368	0.7	21	0.414	0.0	20	0.808
log β-glucosidase	14.0	21	**0.000**	2.5	21	0.115	5.0	21	**0.025**	0.5	20	0.463	1.1	20	0.293	1.2	20	0.278	0.0	20	0.830
Phenol oxidase	16.4	22	**0.000**	7.8	22	**0.005**	7.4	22	**0.007**	2.8	20	0.093	0.1	20	0.787	4.7	20	**0.031**	4.4	20	**0.036**
Peroxidase	6.4	23	**0.011**	0.0	23	0.889	3.1	23	0.079	5.9	21	**0.015**	2.4	21	0.123	2.1	21	0.147	4.5	20	**0.035**

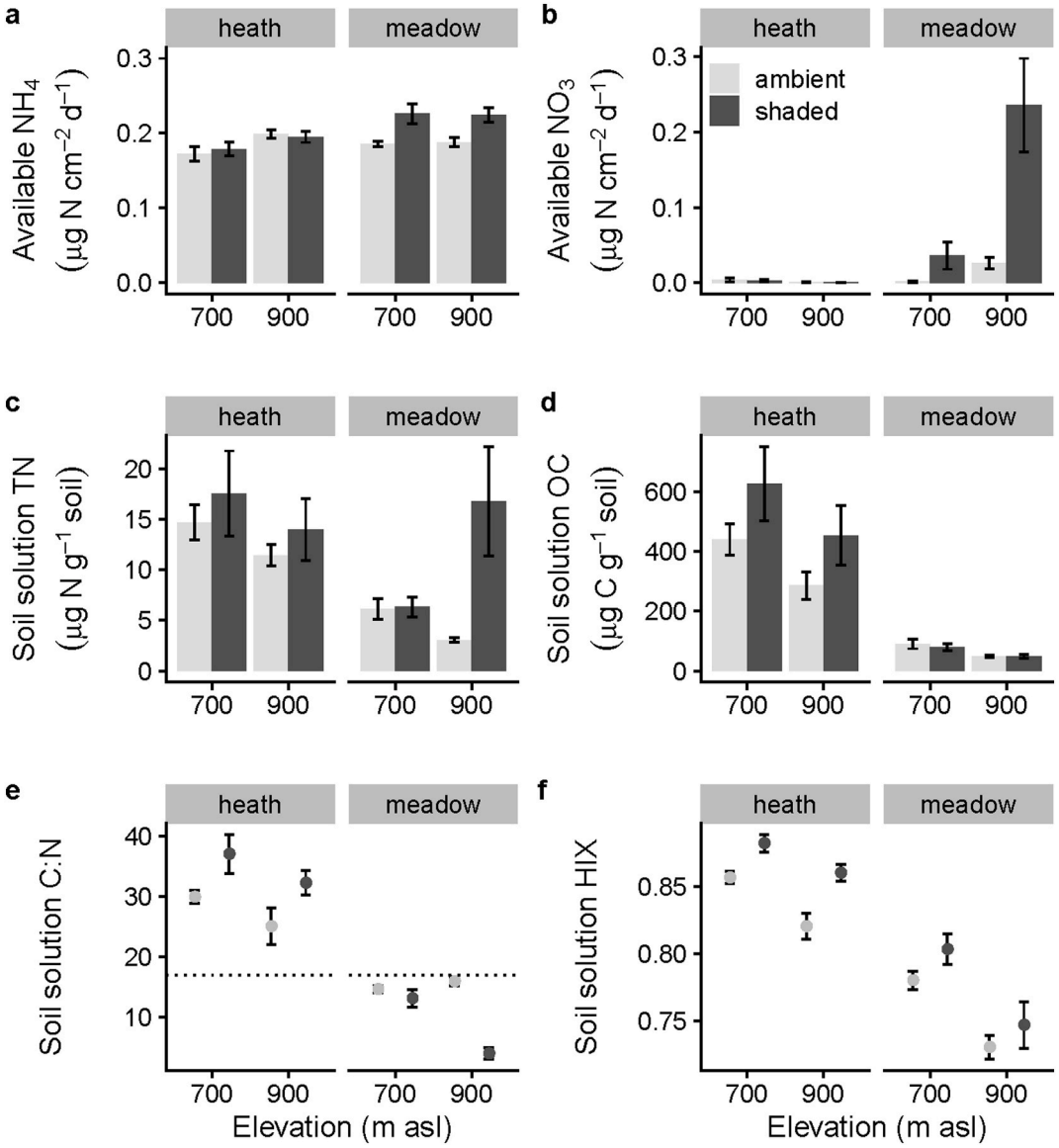

Fig. 2. Biogeochemical responses to experimental shading (dark vs clear grey bars and symbols) for two vegetation types growing at two elevations above the natural treeline. Ammonium (**a**) and nitrate (**b**) availabilities in the soil during the plant growing season were estimated with ion exchange resin bags. Total N (**c**) and organic carbon (**d**) in soil solution, as well as their ratio (**e**) were obtained by percolating water through a soil column. The extent of decomposition of that dissolved organic matter was assessed by the humification index (**f**). Presented are mean treatment values (±SE, n = 6), for which statistical comparisons are given in Table 2. The horizontal dotted line in (**e**) indicates the stoichiometric limit between substrate C- (below) and N- (above) limitation for microbial growth (as in Mooshammer et al., 2014b).

were stronger at the low elevation site (Fig. 4e, Table 2). Shading consistently increased the hydrolytic enzyme activity of fluorescein diacetate and β-glucosidase at both elevations and vegetation types and the meadow had higher β-glucosidase activity than the heath (Fig. 4f–g, Table 2). Activities of the oxidative enzymes phenol oxidase and peroxidase were generally higher in meadow than in heath, and the greatest activity was at the high elevation meadow site (Fig. 4h–i, Table 2). In the meadows, shading had a negative effect on oxidative enzyme activities at the high elevation sites but a positive effect at the low elevation sites, whereas in the heath, shading consistently reduced only the activity of phenol oxidase (Fig. 4h, Table 2).

3.4. Above- and belowground linkages

Through structural equation modelling, we determined the main pathways in which tundra elevation and vegetation interact with their microbiome to constrain the belowground ecosystem potential for carbon storage (Fig. 5, Fig. S4). Shading, despite its pronounced effect on plant productivity and on various soil solution parameters (Fig. 2, Table 2), was not retained in the final SEM. Compared to heath, meadow vegetation type strongly decreased microbial biomass either directly (path = −0.73) or through a cascade of microbial community and physiological parameters, which ultimately constrained the size of the microbial pool by the its carbon use efficiency (path = 0.30). In turn, microbial biomass was the strongest predictor (path = 0.64) of SOC, followed by vegetation type (path = −0.38) and elevation (path = 0.09). The effect of elevation (i.e., the inverse of temperature) on SOM was further mediated through those microbial physiology parameters.

4. Discussion

In this study, we show how tundra primary productivity, vegetation type and elevation interactively determine the ecosystem potential for carbon cycling through a suite of above- and belowground mechanisms.

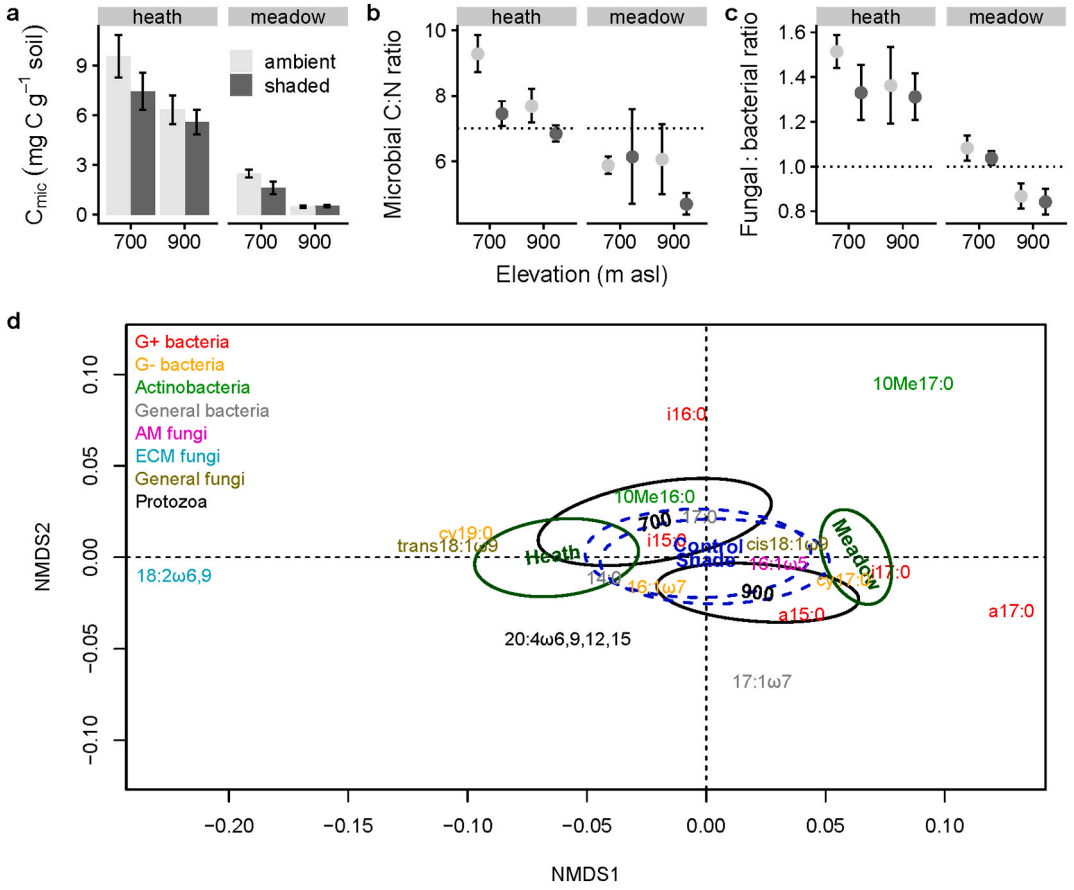

Fig. 3. Size and composition of soil microbial communities. Microbial biomass C (**a**) and its C:N ratio (**b**), as estimated by chloroform fumigation. The relative proportion of fungal to bacterial biomass in the soil against a 1:1 line (**c**), as well as the microbial community structure in a two-dimensional NMDS (**d**) were determined by the PLFA technique. Individual colour-coded markers (**d**) were attributed to broad microbial groups with reference to recent literature (see Methods). Non-overlapping solid circles (SE for site scores per treatment) represent significant ($P < 0.05$) results of PERMANOVA tests performed on Bray-Curtis site dissimilarities. Dashed circles are not significant. For **a** – **c**, presented are mean treatment values (±SE, n = 6), for which statistical comparisons are given in Table 2. Horizontal dotted line in (**b**) indicates the stoichiometric limit between microbial biomass C- (below) and N- (above) growth limitation (as in Mooshammer et al., 2014b). (For interpretation of the references to colour in this figure legend, the reader is referred to the Web version of this article.)

We found consistent patterns in ecosystem processes indicative of SOM accumulation within heath compared to meadow communities across elevations, and a pivotal role of plant productivity therein. The latter was particularly pronounced within meadows, where a sustained photosynthate supply belowground was essential to offset rhizomicrobial C-limitation. Below we explore the additive and interactive responses and feedbacks of plant-soil-microbial linkages and how these relate to prevailing climate regimes across the two studied elevations.

4.1. Belowground ecosystem functioning across two mountain tundra vegetation types

The contrast between herb-dominated meadow and shrub-dominated heath was a major determinant of tundra soil and microbial composition and biogeochemical functioning and, as hypothesised, underpinned the ecosystem potential for C storage. Similar to previous studies comparing woody versus herbaceous vegetation types within the same climatic zones (Hagedorn et al., 2019; Mayor et al., 2017; Sundqvist et al., 2011), we found consistently greater above- and belowground C stocks in the heath than in the meadow. It is likely that this was not the result of higher ecosystem productivity, since previous work has shown that woody and herbaceous vegetation exhibit similar rates of gross ecosystem productivity across the Arctic (Cahoon et al., 2012) and that dominant heath vegetation such as *Empetrum hermaphroditum* has limited contribution to overall GEP rates in tundra ecosystems (Sundqvist et al., 2020). Despite our study being limited to one site and one season, our peak growing season data on potential GEP (Table 1, Fig. S2a) corroborate these previous observations, indicating an even lower rate of atmospheric CO_2 fixation in heath than in meadow, independent of elevation. This suggests that under optimal conditions during the plant growing season the rate of decomposition and microbial turnover, rather than of plant productivity, could play a central role for belowground C storage potential of these two vegetation types.

Our mechanistic approach provided further evidence that belowground abiotic and biotic linkages with vegetation type drive tundra SOC cycling (Fig. 5). Soil temperature was less coupled to atmospheric temperature under shrubs compared to meadow, which is in line with previous work demonstrating cooler microclimate under shrubs (Myers-Smith and Hik, 2013). This temperature buffering in heath reduced microbial physiological responses to warmer conditions at low elevation and, as a consequence, respiration rates and enzymatic activities there did not increase in a similar way as in the meadow. We further demonstrate that lower N availability, as well as higher soil C:N ratios and degree of organic matter humification in heath relative to meadow soils, favours fungal-dominated communities with lower substrate respiration rates and a lower activity of C-degrading extracellular enzymes. This is likely driven by the typically low quality above (Cornelissen et al., 2007) and belowground (Freschet et al., 2013) plant litter inputs in heath compared to meadow ecosystems, which ultimately

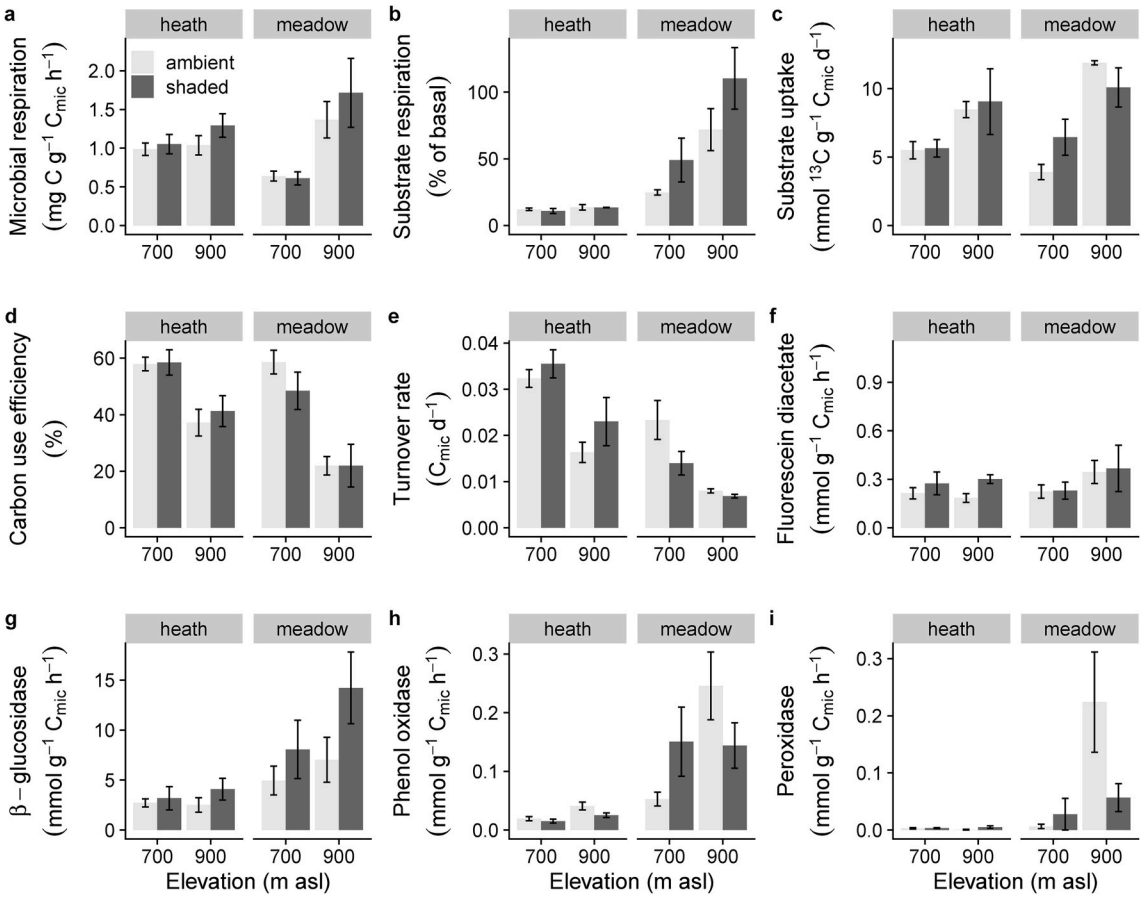

Fig. 4. Microbial biomass-specific rates of main physiological processes: heterotrophic respiration (**a**); ^{13}C-labelled glucose respiration relative to water-addition controls (**b**); ^{13}C-labelled glucose incorporation into the sum of all quantified PLFA (including therein the general markers 16:0, 18:0 and 20:0, which do not contribute to any of the main groups (Schnecker et al., 2012) presented in Fig. 3c); carbon use efficiency (**d**); biomass turnover rate (**e**); and the extracellular enzymatic activity of fluorescein diacetate (**f**); β-glucosidase (**g**); phenol oxidase (**h**); and peroxidase (**i**). Presented are mean treatment values (±SE, n = 6), for which statistical comparisons are given in Table 2.

determine the rates of SOM cycling. More specifically, in contrast to meadows, both soil and soil solution C:N ratios in heath were higher than the 17:1 mass-based ratio, above which microbial N-limitation generally occurs (Mooshammer et al., 2014b). This was further reflected in the microbial biomass C:N ratio (i.e., >7:1), indicative of N growth limitation (Mooshammer et al., 2014b). Our data thus support the concept that a suite of microbial community properties, which drive soil formation (i.e., biomass, community composition, physiology), dependon the overlying vegetation and are critical for understanding biogeochemical cycles (Crowther et al., 2019).

4.2. *Belowground ecosystem functioning across two mountain tundra elevations*

The effects of warmer atmospheric temperatures across the two elevations (in this study, *ca.* +1.9 K) on biogeochemistry and microbial physiology were numerous, but the hypothesised acceleration of C and N cycles at the low elevation was not confirmed. On the contrary, mass-specific rates of microbial respiration decreased and those of growth (i.e., turnover) increased with warmer temperatures at low elevation, resulting in a particularly high (*ca.* 60%) CUE (Manzoni et al., 2012; Sinsabaugh et al., 2016). Furthermore, per unit biomass, low elevation microbes produced less oxidative enzymes for the degradation of complex biopolymers, and showed lower rates of glucose mineralisation and uptake. In line with these observations, we found that total pools of soil and microbial C and N were larger at the low elevation, whereas growing season N-availability was smaller. This was paralleled by an accumulation of SOM with a high degree of humification and a high C:N ratio, which are both indicative for nutrient-limited conditions in tundra ecosystems (Mack et al., 2004; Schmidt et al., 2002). Alongside this, independent of vegetation type, soils at low elevation had fungal-dominated microbial communities with higher biomass C:N ratios. As fungal-dominated communities imply slow elemental cycling (Bardgett et al., 2005), they potentially modulated the effect of warmer atmospheric temperatures at the low elevation site. Their typically high biomass C:N (Strickland and Rousk, 2010) and high CUE (Geyer et al., 2016; Malik et al., 2016) have likely contributed to a long-term SOM storage within extensive mycelial networks (Clemmensen et al., 2013, 2015). It is thus plausible that the measured larger microbial biomass in these fungal-dominated communities, with lower respiratory losses and faster turnover rates, provided a greater supply of organic residues and favoured the accumulation of stable SOM forms. This process could have further been enhanced by the proximity of mineral surfaces in these shallow mountain tundra soils, which is known to facilitate long-term SOM storage through its association with mineral particles (Bradford et al., 2016; Cotrufo et al., 2013; Lavallee et al., 2020; Liang et al., 2017). Altogether, the combined increase at lower elevation in belowground carbon inputs, through higher rates of GEP and microbial turnover, contributed to the greater accumulation of SOM stocks, suggesting of a sustained C sink function of tundra soils with moderately warmer temperatures at this study site.

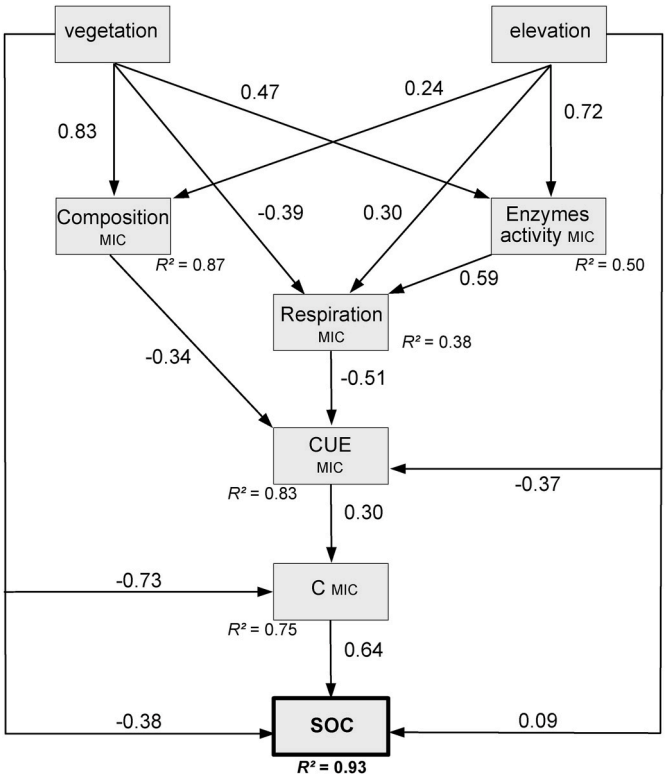

Fig. 5. Structural equation model of plant-soil-microbial linkages in tundra ecosystems. Arrows indicate significant ($P < 0.05$) paths between variables retained in the final model. The numbers associated with each arrow show the standardized parameter estimates (i.e., standardized regression weights). Square multiple correlations (R^2 values) for the predicted factor are indicated besides the dependent variable. Model fits are on average good (Fisher's C = 39.3, $P = 0.177$, df = 32).

4.3. Belowground ecosystem responses to altered plant productivity across vegetation types and elevation

The supply of plant photosynthetic assimilates belowground (i.e., ambient vs. shaded treatment) was, as hypothesised, fundamental for overcoming substrate limitation of tundra microbial communities. Even during the limited duration of a single growing season, primary productivity exerted strong positive effects on the size of the microbial pool and its metabolic functions. This was likely driven by a shift from below- to aboveground plant C-allocation strategies with experimental shading (Möhl et al., 2019), in turn, causing microbial C-limitation (Mikola et al., 2000). Substrate limitation was greatest at the low elevation, where microbial biomass strongly depended on plant photosynthates, as well as in the meadows, where bacterial-dominated communities were particularly constrained by the low SOM stocks and C:N ratios. Furthermore, we found no evidence for stimulated SOM decomposition rates with increased tundra ecosystem productivity due to rhizosphere priming effects (e.g., Hartley et al., 2012). To the contrary, in comparison to the shaded treatment, under ambient light, we observed lower SOM humification, matched by a decreased microbial enzymatic activity and lower DOCfor both meadow and heath soils. Likewise, we found no compelling evidence for a potential increase in nitrogen mineralisation due to microbial nutrient mining of SOM, resulting from a greater N-demand with increased plant productivity (e.g., Chen et al., 2014; Zak et al., 2019). Instead, in the meadow, N was likely not a growth limiting factor for microbes, as both their substrate (soil and soil solution) and biomass had characteristically C-limiting low C:N ratios (Manzoni et al., 2012; Mooshammer et al., 2014b). As a result, in the absence of photosynthates (i.e., under shading), the availability of ammonium and nitrate in meadow soils increased and microbial biomass C:N decreased, providing evidence for a physiological adjustment of microbes in response to C-limitation (Mooshammer et al., 2014a) and possibly a stimulation of ammonium nitrification in the absence of plant competition for N (Jonasson et al., 1999; Mikola et al., 2000). Even though the heath had more N-limiting conditions with substantially higher soil and soil solution C:N ratios than did the meadow, microbes in the heath similarly reduced their biomass and C:N ratios in response to shading without affecting the seasonal fluxes of ammonium and nitrate in the soil. These findings suggest that tundra plant C-supply belowground is a strong prerequisite of SOM build-up above the treeline, yet its fundamental effect remained masked in this (short-term) study by the prevailing (a)biotic conditions across tundra vegetation types and elevation-dependent climate regimes. Further mechanistic studies directly manipulating plant productivity (i.e. through shading, girdling, defoliation), rather than inferring it from comparisons among vegetation types and standing biomass, are needed from across the tundra region in order to draw a comprehensive picture of climate change effects on SOM cycling.

4.4. Conclusions

Altogether, our results demonstrate that consistent structural and physiological adaptations in soil microbial communities across elevations and vegetation types underpin ecosystem functioning and its potential for C storage in this mountain tundra system. We show that belowground photosynthetic inputs by plants limit the enzymatic SOM decomposition, likely by alleviating microbial C demand. This effect is sustained with warmer temperature and higher plant productivity at lower elevation, where a microbial community shift towards a fungal energy channel with high CUE further contributes to the observed increase in belowground C pools. Similarly, tundra heath vegetation with its associated fungal-dominated microbial communities retards rates of soil C cycling and ultimately leads to higher ecosystem C stocks. We thus argue that, owing to these cascading above- and belowground linkages, plant community characteristics (i.e. productivity and vegetation type) could potentially serve as reliable predictors of ecosystem C storage potential in mountain tundra ecosystems.

Author contributions

K.G., R.M. and T.W. designed the study; K.G., M.S., E.D. and D.W. chose the experimental sites; and K.G. collected field data and processed soil samples with help from R.M. In the lab, K.G. did soil ^{13}C enrichment, respiration measurements and PLFA extractions; A.C. quantified $\delta^{13}C$-PLFA with help from A.R.; M.V. performed extracellular enzymatic activity assays with help from V.J.; T.W. determined microbial physiology metrics with help from A.R. K.G. and T.W. analysed the data and V.J. did the SEM. K.G. wrote the manuscript with substantial contributions from all authors.

Data availability

The data that support the findings of this study are available from the corresponding author upon reasonable request.

Declaration of competing interest

The authors declare that they have no known competing financial interests or personal relationships that could have appeared to influence the work reported in this paper.

Acknowledgements

We thank Laurenz Teuber for technical lab assistance at the Climate Impacts Research Centre (CIRC) in Abisko. The interns Katharina

Krumpholz, Luise Pabst and Johannes Moeser provided valuable support in the field. The study benefitted from internal CIRC funding for the use of the Abisko Scientific Research Station, kindly operated by the Swedish Polar Research Secretariat. K.G. was further supported by funding from the Swiss National Science Foundation (grant no. PZ00P2_174047).

Appendix A. Supplementary data

Supplementary data to this article can be found online at https://doi.org/10.1016/j.soilbio.2021.108530.

References

Bahn, M., Lattanzi, F.A., Hasibeder, R., Wild, B., Koranda, M., Danese, V., Brüggemann, N., Schmitt, M., Siegwolf, R., Richter, A., 2013. Responses of belowground carbon allocation dynamics to extended shading in mountain grassland. New Phytologist 198, 116–126. https://doi.org/10.1111/nph.12138.

Baldrian, P., 2014. Distribution of extracellular enzymes in soils: spatial heterogeneity and determining factors at various scales. Soil Science Society of America Journal 78, 11–18. https://doi.org/10.2136/sssaj2013.04.0155dgs.

Bardgett, R.D., Bowman, W.D., Kaufmann, R., Schmidt, S.K., 2005. A temporal approach to linking aboveground and belowground ecology. Trends in Ecology & Evolution 20, 634–641. https://doi.org/10.1016/j.tree.2005.08.005.

Bergmann, J., Weigelt, A., van der Plas, F., Laughlin, D.C., Kuyper, T.W., Guerrero-Ramirez, N., Valverde-Barrantes, O.J., Bruelheide, H., Freschet, G.T., Iversen, C.M., Kattge, J., McCormack, M.L., Meier, I.C., Rillig, M.C., Roumet, C., Semchenko, M., Sweeney, C.J., van Ruijven, J., York, L.M., Mommer, L., 2020. The fungal collaboration gradient dominates the root economics space in plants. Science Advances 6. https://doi.org/10.1126/sciadv.aba3756 eaba3756.

Björk, R.G., Klemedtsson, L., Molau, U., Harndorf, J., Ödman, A., Giesler, R., 2007. Linkages between N turnover and plant community structure in a tundra landscape. Plant and Soil 294, 247–261. https://doi.org/10.1007/s11104-007-9250-4.

Bjorkman, A.D., Myers-Smith, I.H., Elmendorf, S.C., Normand, S., Rüger, N., Beck, P.S.A., Blach-Overgaard, A., Blok, D., Cornelissen, J.H.C., Forbes, B.C., Georges, D., Goetz, S.J., Guay, K.C., Henry, G.H.R., HilleRisLambers, J., Hollister, R.D., Karger, D. N., Kattge, J., Manning, P., Prevéy, J.S., Rixen, C., Schaepman-Strub, G., Thomas, H. J.D., Vellend, M., Wilmking, M., Wipf, S., Carbognani, M., Hermanutz, L., Lévesque, E., Molau, U., Petraglia, A., Soudzilovskaia, N.A., Spasojevic, M.J., Tomaselli, M., Vowles, T., Alatalo, J.M., Alexander, H.D., Anadon-Rosell, A., Angers-Blondin, S., Beest, M. te, Berner, L., Björk, R.G., Buchwal, A., Buras, A., Christie, K., Cooper, E.J., Dullinger, S., Elberling, B., Eskelinen, A., Frei, E.R., Grau, O., Grogan, P., Hallinger, M., Harper, K.A., Heijmans, M.M.P.D., Hudson, J., Hülber, K., Iturrate-Garcia, M., Iversen, C.M., Jaroszynska, F., Johnstone, J.F., Jørgensen, R.H., Kaarlejärvi, E., Klady, R., Kuleza, S., Kulonen, A., Lamarque, L.J., Lantz, T., Little, C. J., Speed, J.D.M., Michelsen, A., Milbau, A., Nabe-Nielsen, J., Nielsen, S.S., Ninot, J. M., Oberbauer, S.F., Olofsson, J., Onipchenko, V.G., Rumpf, S.B., Semenchuk, P., Shetti, R., Collier, L.S., Street, L.E., Suding, K.N., Tape, K.D., Trant, A., Treier, U.A., Tremblay, J.P., Tremblay, M., Venn, S., Weijers, S., Zamin, T., Boulanger-Lapointe, N., Gould, W.A., Hik, D.S., Hofgaard, A., Jónsdóttir, I.S., Jorgenson, J., Klein, J., Magnusson, B., Tweedie, C., Wookey, P.A., Bahn, M., Blonder, B., van Bodegom, P.M., Bond-Lamberty, B., Campetella, G., Cerabolini, B.E.L., Chapin, F.S., Cornwell, W.K., Craine, J., Dainese, M., de Vries, F.T., Díaz, S., Enquist, B.J., Green, W., Milla, R., Niinemets, Ü., Onoda, Y., Ordoñez, J.C., Ozinga, W.A., Penuelas, J., Poorter, H., Poschlod, P., Reich, P.B., Sandel, B., Schamp, B., Sheremetev, S., Weiher, E., 2018. Plant functional trait change across a warming tundra biome. Nature 562, 57–62. https://doi.org/10.1038/s41586-018-0563-7.

Blume-Werry, G., Lindén, E., Andresen, L., Classen, A.T., Sanders, N.J., von Oppen, J., Sundqvist, M.K., 2018. Proportion of fine roots, but not plant biomass allocation below ground, increases with elevation in arctic tundra. Journal of Vegetation Science 29, 226–235. https://doi.org/10.1111/jvs.12605.

Bradford, M.A., Wieder, W.R., Bonan, G.B., Fierer, N., Raymond, P.A., Crowther, T.W., 2016. Managing uncertainty in soil carbon feedbacks to climate change. Nature Climate Change 6, 751–758. https://doi.org/10.1038/nclimate3071.

Cahoon, S.M.P., Sullivan, P.F., Shaver, G.R., Welker, J.M., Post, E., 2012. Interactions among shrub cover and the soil microclimate may determine future Arctic carbon budgets. Ecology Letters 15, 1415–1422. https://doi.org/10.1111/j.1461-0248.2012.01865.x.

Callaghan, T.V., Jonasson, C., Thierfelder, T., Yang, Z., Hedenås, H., Johansson, M., Molau, U., Van Bogaert, R., Michelsen, A., Olofsson, J., Gwynn-Jones, D., Bokhorst, S., Phoenix, G., Bjerke, J.W., Tømmervik, H., Christensen, T.R., Hanna, E., Koller, E.K., Sloan, V.L., 2013. Ecosystem change and stability over multiple decades in the Swedish subarctic: complex processes and multiple drivers. Philosophical Transactions of the Royal Society B: Biological Sciences 368, 20120488. https://doi.org/10.1098/rstb.2012.0488.

Chen, R., Senbayram, M., Blagodatsky, S., Myachina, O., Dittert, K., Lin, X., Blagodatskaya, E., Kuzyakov, Y., 2014. Soil C and N availability determine the priming effect: microbial N mining and stoichiometric decomposition theories. Global Change Biology 20, 2356–2367. https://doi.org/10.1111/gcb.12475.

Clemmensen, K.E., Bahr, A., Ovaskainen, O., Dahlberg, A., Ekblad, A., Wallander, H., Stenlid, J., Finlay, R.D., Wardle, D.A., Lindahl, B.D., 2013. Roots and associated fungi drive long-term carbon sequestration in boreal forest. Science 339, 1615–1618. https://doi.org/10.1126/science.1231923.

Clemmensen, K.E., Durling, M.B., Michelsen, A., Hallin, S., Finlay, R.D., Lindahl, B.D., 2021. A tipping point in carbon storage when forest expands into tundra is related to mycorrhizal recycling of nitrogen. Ecol. Letters ele 13735. https://doi.org/10.1111/ele.13735.

Clemmensen, K.E., Finlay, R.D., Dahlberg, A., Stenlid, J., Wardle, D.A., Lindahl, B.D., 2015. Carbon sequestration is related to mycorrhizal fungal community shifts during long-term succession in boreal forests. New Phytologist 205, 1525–1536. https://doi.org/10.1111/nph.13208.

Cornelissen, J.H.C., Van Bodegom, P.M., Aerts, R., Callaghan, T.V., Van Logtestijn, R.S. P., Alatalo, J., Stuart Chapin, F., Gerdol, R., Gudmundsson, J., Gwynn-Jones, D., Hartley, A.E., Hik, D.S., Hofgaard, A., Jónsdóttir, I.S., Karlsson, S., Klein, J.A., Laundre, J., Magnusson, B., Michelsen, A., Molau, U., Onipchenko, V.G., Quested, H. M., Sandvik, S.M., Schmidt, I.K., Shaver, G.R., Solheim, B., Soudzilovskaia, N.A., Stenström, A., Tolvanen, A., Totland, Ø., Wada, N., Welker, J.M., Zhao, X., Brancaleoni, Lisa, Brancaleoni, Laura, De Beus, M.A.H., Cooper, E.J., Dalen, L., Harte, J., Hobbie, S.E., Hoefsloot, G., Jägerbrand, A., Jonasson, S., Lee, J.A., Lindblad, K., Melillo, J.M., Neill, C., Press, M.C., Rozema, J., Zielke, M., 2007. Global negative vegetation feedback to climate warming responses of leaf litter decomposition rates in cold biomes. Ecology Letters 10, 619–627. https://doi.org/10.1111/j.1461-0248.2007.01051.x.

Cotrufo, M.F., Wallenstein, M.D., Boot, C.M., Denef, K., Paul, E., 2013. The Microbial Efficiency-Matrix Stabilization (MEMS) framework integrates plant litter decomposition with soil organic matter stabilization: do labile plant inputs form stable soil organic matter? Global Change Biology 19, 988–995. https://doi.org/10.1111/gcb.12113.

Criquet, S., Tagger, S., Vogt, G., Iacazio, G., Le Petit, J., 1999. Laccase activity of forest litter. Soil Biology and Biochemistry 31, 1239–1244. https://doi.org/10.1016/S0038-0717(99)00038-3.

Crowther, T.W., van den Hoogen, J., Wan, J., Mayes, M.A., Keiser, A.D., Mo, L., Averill, C., Maynard, D.S., 2019. The Global Soil Community and its Influence on Biogeochemistry. Science 365. https://doi.org/10.1126/science.aav0550 eaav0550.

Dorrepaal, E., 2007. Are plant growth-form-based classifications useful in predicting northern ecosystem carbon cycling feedbacks to climate change? Journal of Ecology 95, 1167–1180. https://doi.org/10.1111/j.1365-2745.2007.01294.x.

Elmendorf, S.C., Henry, G.H.R., Hollister, R.D., Fosaa, A.M., Gould, W.A., Hermanutz, L., Hofgaard, A., Jónsdóttir, I.S., Jorgenson, J.C., Lévesque, E., Magnusson, B., Molau, U., Myers-Smith, I.H., Oberbauer, S.F., Rixen, C., Tweedie, C.E., Walker, M. D., 2015. Experiment, monitoring, and gradient methods used to infer climate change effects on plant communities yield consistent patterns. Proceedings of the National Academy of Sciences 112, 448–452. https://doi.org/10.1073/pnas.1410088112.

Fontaine, S., Barot, S., Barré, P., Bdioui, N., Mary, B., Rumpel, C., 2007. Stability of organic carbon in deep soil layers controlled by fresh carbon supply. Nature 450, 277–280. https://doi.org/10.1038/nature06275.

Freschet, G.T., Cornwell, W.K., Wardle, D.A., Elumeeva, T.G., Liu, W., Jackson, B.G., Onipchenko, V.G., Soudzilovskaia, N.A., Tao, J., Cornelissen, J.H.C., 2013. Linking litter decomposition of above- and below-ground organs to plant-soil feedbacks worldwide. Journal of Ecology 101, 943–952. https://doi.org/10.1111/1365-2745.12092.

Frey, S.D., 2019. Mycorrhizal fungi as mediators of soil organic matter dynamics. Ann. Rev. Ecol. Evol. and Sys. 50, 237–259. https://doi.org/10.1146/annurev-ecolsys-110617-062331.

Fuchslueger, L., Bahn, M., Fritz, K., Hasibeder, R., Richter, A., 2014. Experimental drought reduces the transfer of recently fixed plant carbon to soil microbes and alters the bacterial community composition in a mountain meadow. New Phytologist 201, 916–927. https://doi.org/10.1111/nph.12569.

Gavazov, K., Mills, R., Spiegelberger, T., Lenglet, J., Buttler, A., 2014. Biotic and abiotic constraints on the decomposition of fagus sylvatica leaf litter along an altitudinal gradient in contrasting land-use types. Ecosystems 17, 1326–1337. https://doi.org/10.1007/s10021-014-9798-9.

Geyer, K.M., Kyker-Snowman, E., Grandy, A.S., Frey, S.D., 2016. Microbial carbon use efficiency: accounting for population, community, and ecosystem-scale controls over the fate of metabolized organic matter. Biogeochemistry 127, 173–188. https://doi.org/10.1007/s10533-016-0191-y.

Grace, J.B., Adler, P.B., Stanley Harpole, W., Borer, E.T., Seabloom, E.W., 2014. Causal networks clarify productivity-richness interrelations, bivariate plots do not. Functional Ecology 28, 787–798. https://doi.org/10.1111/1365-2435.12269.

Grace, J.B., Anderson, T.M., Seabloom, E.W., Borer, E.T., Adler, P.B., Harpole, W.S., Hautier, Y., Hillebrand, H., Lind, E.M., Pärtel, M., Bakker, J.D., Buckley, Y.M., Crawley, M.J., Damschen, E.I., Davies, K.F., Fay, P.A., Firn, J., Gruner, D.S., Hector, A., Knops, J.M.H., MacDougall, A.S., Melbourne, B.A., Morgan, J.W., Orrock, J.L., Prober, S.M., Smith, M.D., 2016. Integrative modelling reveals mechanisms linking productivity and plant species richness. Nature 529, 390–393. https://doi.org/10.1038/nature16524.

Gunina, A., Kuzyakov, Y., 2015. Sugars in soil and sweets for microorganisms: review of origin, content, composition and fate. Soil Biology and Biochemistry 90, 87–100. https://doi.org/10.1016/j.soilbio.2015.07.021.

Hagedorn, F., Gavazov, K., Alexander, J.M., 2019. Above- and belowground linkages shape responses of mountain vegetation to climate change. Science 365, 1119–1123. https://doi.org/10.1126/science.aax4737.

Hagedorn, F., Mulder, J., Jandl, R., 2010. Mountain soils under a changing climate and land-use. Biogeochemistry 97, 1–5. https://doi.org/10.1007/s10533-009-9386-9.

Hartley, I.P., Garnett, M.H., Sommerkorn, M., Hopkins, D.W., Fletcher, B.J., Sloan, V.L., Phoenix, G.K., Wookey, P.A., 2012. A potential loss of carbon associated with greater

plant growth in the European Arctic. Nature Climate Change 2, 875–879. https://doi.org/10.1038/nclimate1575.
Hill, P., Kuzyakov, Y., Jones, D., Farrar, J., 2007. Response of root respiration and root exudation to alterations in root C supply and demand in wheat. Plant and Soil 291, 131–141. https://doi.org/10.1007/s11104-006-9180-6.
Hobbie, S.E., Schimel, J.P., Trumbore, S.E., Randerson, J.R., 2000. Controls over carbon storage and turnover in high-latitude soils. Global Change Biology 6, 196–210. https://doi.org/10.1046/j.1365-2486.2000.06021.x.
Högberg, M.N., Briones, M.J.I., Keel, S.G., Metcalfe, D.B., Campbell, C., Midwood, A.J., Thornton, B., Hurry, V., Linder, S., Näsholm, T., Högberg, P., 2010. Quantification of effects of season and nitrogen supply on tree below-ground carbon transfer to ectomycorrhizal fungi and other soil organisms in a boreal pine forest. New Phytologist 187, 485–493. https://doi.org/10.1111/j.1469-8137.2010.03274.x.
Jassey, V.E.J., Chiapusio, G., Gilbert, D., Toussaint, M.L., Binet, P., 2012. Phenoloxidase and peroxidase activities in Sphagnum-dominated peatland in a warming climate. Soil Biology and Biochemistry 46, 49–52. https://doi.org/10.1016/j.soilbio.2011.11.011.
Jassey, V.E.J., Reczuga, M.K., Zielińska, M., Słowińska, S., Robroek, B.J.M., Mariotte, P., Seppey, C.V.W., Lara, E., Barabach, J., Słowiński, M., Bragazza, L., Chojnicki, B.H., Lamentowicz, M., Mitchell, E.A.D., Buttler, A., 2018. Tipping point in plant–fungal interactions under severe drought causes abrupt rise in peatland ecosystem respiration. Global Change Biology 24, 972–986. https://doi.org/10.1111/gcb.13928.
Jonasson, S., Michelsen, A., Schmidt, I.K., Nielsen, E.V., 1999. Responses in microbes and plants to changed temperature, nutrient, and light regimes in the arctic. Ecology 80, 1828. https://doi.org/10.2307/176661.
Kaiser, C., Frank, A., Wild, B., Koranda, M., Richter, A., 2010a. Negligible contribution from roots to soil-borne phospholipid fatty acid fungal biomarkers 18:2ω6,9 and 18:1ω9. Soil Biology and Biochemistry 42, 1650–1652. https://doi.org/10.1016/j.soilbio.2010.05.019.
Kaiser, C., Koranda, M., Kitzler, B., Fuchslueger, L., Schnecker, J., Schweiger, P., Rasche, F., Zechmeister-Boltenstern, S., Sessitsch, A., Richter, A., 2010b. Belowground carbon allocation by trees drives seasonal patterns of extracellular enzyme activities by altering microbial community composition in a beech forest soil. New Phytologist 187, 843–858. https://doi.org/10.1111/j.1469-8137.2010.03321.x.
Karhu, K., Auffret, M.D., Dungait, J.A.J., Hopkins, D.W., Prosser, J.I., Singh, B.K., Subke, J.A., Wookey, P.A., Agren, G.I., Sebastià, M.T., Gouriveau, F., Bergkvist, G., Meir, P., Nottingham, A.T., Salinas, N., Hartley, I.P., 2014. Temperature sensitivity of soil respiration rates enhanced by microbial community response. Nature 513, 81–84. https://doi.org/10.1038/nature13604.
Keiluweit, M., Bougoure, J.J., Nico, P.S., Pett-Ridge, J., Weber, P.K., Kleber, M., 2015. Mineral protection of soil carbon counteracted by root exudates. Nature Climate Change 5, 588–595. https://doi.org/10.1038/nclimate2580.
Körner, C., 2007. The use of "altitude" in ecological research. Trends in Ecology & Evolution 22, 569–574. https://doi.org/10.1016/j.tree.2007.09.006.
Kuzyakov, Y., 2006. Sources of CO2 efflux from soil and review of partitioning methods. Soil Biology and Biochemistry 38, 425–448. https://doi.org/10.1016/j.soilbio.2005.08.020.
Lavallee, J.M., Soong, J.L., Cotrufo, M.F., 2020. Conceptualizing soil organic matter into particulate and mineral-associated forms to address global change in the 21st century. Global Change Biology 26, 261–273. https://doi.org/10.1111/gcb.14859.
Lefcheck, J.S., 2016. piecewiseSEM: piecewise structural equation modelling in r for ecology, evolution, and systematics. Meth. Ecol. Evol. 7, 573–579. https://doi.org/10.1111/2041-210X.12512.
Liang, C., Schimel, J.P., Jastrow, J.D., 2017. The importance of anabolism in microbial control over soil carbon storage. Nat. Microbiol. 2, 1–6. https://doi.org/10.1038/nmicrobiol.2017.105.
Mack, M.C., Schuur, E.A.G., Bret-Harte, M.S., Shaver, G.R., Chapin, F.S., 2004. Ecosystem carbon storage in arctic tundra reduced by long-term nutrient fertilization. Nature 431, 440–443. https://doi.org/10.1038/nature02887.
Malik, A.A., Chowdhury, S., Schlager, V., Oliver, A., Puissant, J., Vazquez, P.G.M., Jehmlich, N., von Bergen, M., Griffiths, R.I., Gleixner, G., 2016. Soil fungal: bacterial ratios are linked to altered carbon cycling. Frontiers in Microbiology 7, 1–11. https://doi.org/10.3389/fmicb.2016.01247.
Manzoni, S., Taylor, P., Richter, A., Porporato, A., Ågren, G.I., 2012. Environmental and stoichiometric controls on microbial carbon-use efficiency in soils. New Phytologist 196, 79–91. https://doi.org/10.1111/j.1469-8137.2012.04225.x.
Mayor, J.R., Sanders, N.J., Classen, A.T., Bardgett, R.D., Clément, J.C., Fajardo, A., Lavorel, S., Sundqvist, M.K., Bahn, M., Chisholm, C., Cieraad, E., Gedalof, Z., Grigulis, K., Kudo, G., Oberski, D.L., Wardle, D.A., 2017. Elevation alters ecosystem properties across temperate treelines globally. Nature 542, 91–95. https://doi.org/10.1038/nature21027.
Mikola, J., Barker, G.M., Wardle, D.A., 2000. Linking above-ground and below-ground effects in autotrophic microcosms: effects of shading and defoliation on plant and soil properties. Oikos 89, 577–587. https://doi.org/10.1034/j.1600-0706.2000.890318.x.
Möhl, P., Hiltbrunner, E., Körner, C., 2019. Halving sunlight reveals no carbon limitation of aboveground biomass production in alpine grassland. Glob. Change Biol. gcb 14949. https://doi.org/10.1111/gcb.14949.
Mooshammer, M., Wanek, W., Hämmerle, I., Fuchslueger, L., Hofhansl, F., Knoltsch, A., Schnecker, J., Takriti, M., Watzka, M., Wild, B., Keiblinger, K.M., Zechmeister-Boltenstern, S., Richter, A., 2014a. Adjustment of microbial nitrogen use efficiency to carbon:nitrogen imbalances regulates soil nitrogen cycling. Nature Communications 5, 1–7. https://doi.org/10.1038/ncomms4694.
Mooshammer, M., Wanek, W., Zechmeister-Boltenstern, S., Richter, A., 2014b. Stoichiometric imbalances between terrestrial decomposer communities and their resources: mechanisms and implications of microbial adaptations to their resources. Frontiers in Microbiology 5, 1–10. https://doi.org/10.3389/fmicb.2014.00022.
Myers-Smith, I.H., Hik, D.S., 2013. Shrub canopies influence soil temperatures but not nutrient dynamics: an experimental test of tundra snow-shrub interactions. Ecology and Evolution 3, 3683–3700. https://doi.org/10.1002/ece3.710.
Ohno, T., 2002. Fluorescence inner-filtering correction for determining the humification index of dissolved organic matter. Environmental Science and Technology 36, 742–746. https://doi.org/10.1021/es0155276.
Oksanen, J., Blanchet, F.G., Friendly, M., Kindt, R., Legendre, P., McGlinn, D., Minchin, P.R., O'Hara, R.B., Simpson, G.L., Solymos, P., Stevens, M.H.H., Szoecs, E., Wagner, H., 2019. Vegan: Community Ecology Package.
Olsson, P.A., 1999. Signature fatty acids provide tools for determination of the distribution and interactions of mycorrhizal fungi in soil. FEMS Microbiology Ecology 29, 303–310. https://doi.org/10.1016/S0168-6496(99)00021-5.
Parker, T.C., Subke, J.-A., Wookey, P.A., 2015. Rapid carbon turnover beneath shrub and tree vegetation is associated with low soil carbon stocks at a subarctic treeline. Global Change Biology 21, 2070–2081. https://doi.org/10.1111/gcb.12793.
Phillips, R.L., Zak, D.R., Holmes, W.E., White, D.C., 2002. Microbial community composition and function beneath temperate trees exposed to elevated atmospheric carbon dioxide and ozone. Oecologia 131, 236–244. https://doi.org/10.1007/s00442-002-0868-x.
Pinheiro, J., Bates, D., DebRoy, S., Sarkar, D., 2018. Linear and Nonlinear Mixed Effects Models. R Core Team, nlme.
Prommer, J., Walker, T.W.N., Wanek, W., Braun, J., Zezula, D., Hu, Y., Hofhansl, F., Richter, A., 2020. Increased microbial growth, biomass, and turnover drive soil organic carbon accumulation at higher plant diversity. Global Change Biology 26, 669–681. https://doi.org/10.1111/gcb.14777.
R Core Team, 2018. R: A Language and Environment for Statistical Computing.
Rinnan, R., Michelsen, A., Bååth, E., Jonasson, S., 2007. Fifteen years of climate change manipulations alter soil microbial communities in a subarctic heath ecosystem. Global Change Biology 13, 28–39. https://doi.org/10.1111/j.1365-2486.2006.01263.x.
Ruess, L., Chamberlain, P.M., 2010. The fat that matters: soil food web analysis using fatty acids and their carbon stable isotope signature. Soil Biology and Biochemistry 42, 1898–1910. https://doi.org/10.1016/j.soilbio.2010.07.020.
Saenger, A., Cécillon, L., Poulenard, J., Bureau, F., De Daniéli, S., Gonzalez, J.M., Brun, J. J., 2015. Surveying the carbon pools of mountain soils: a comparison of physical fractionation and Rock-Eval pyrolysis. Geoderma 241–242, 279–288. https://doi.org/10.1016/j.geoderma.2014.12.001.
Schmidt, I.K., Jonasson, S., Shaver, G.R., Michelsen, A., Nordin, A., 2002. Mineralization and distribution of nutrients in plants and microbes in four arctic ecosystems: responses to warming. Plant and Soil 242, 93–106. https://doi.org/10.1023/A:1019642007929.
Schmitt, A., Pausch, J., Kuzyakov, Y., 2013. Effect of clipping and shading on C allocation and fluxes in soil under ryegrass and alfalfa estimated by 14C labelling. Applied Soil Ecology 64, 228–236. https://doi.org/10.1016/j.apsoil.2012.12.015.
Schnecker, J., Wild, B., Fuchslueger, L., Richter, A., 2012. A field method to store samples from temperate mountain grassland soils for analysis of phospholipid fatty acids. Soil Biology and Biochemistry 51, 81–83. https://doi.org/10.1016/j.soilbio.2012.03.029.
Sinsabaugh, R.L., Turner, B.L., Talbot, J.M., Waring, B.G., Powers, J.S., Kuske, C.R., Moorhead, D.L., Follstad Shah, J.J., 2016. Stoichiometry of microbial carbon use efficiency in soils. Ecological Monographs 86, 172–189. https://doi.org/10.1890/15-2110.1.
Solly, E.F., Djukic, I., Moiseev, P.A., Andreyashkina, N.I., Devi, N.M., Göransson, H., Mazepa, V.S., Shiyatov, S.G., Trubina, M.R., Schweingruber, F.H., Wilmking, M., Hagedorn, F., 2017. Treeline advances and associated shifts in the ground vegetation alter fine root dynamics and mycelia production in the South and Polar Urals. Oecologia 183, 571–586. https://doi.org/10.1007/s00442-016-3785-0.
Streit, K., Hagedorn, F., Hiltbrunner, D., Portmann, M., Saurer, M., Buchmann, N., Wild, B., Richter, A., Wipf, S., Siegwolf, R.T.W., 2014. Soil warming alters microbial substrate use in alpine soils. Global Change Biology 20, 1327–1338. https://doi.org/10.1111/gcb.12396.
Strickland, M.S., Rousk, J., 2010. Considering fungal:bacterial dominance in soils – methods, controls, and ecosystem implications. Soil Biology and Biochemistry 42, 1385–1395. https://doi.org/10.1016/j.soilbio.2010.05.007.
Sundqvist, M.K., Giesler, R., Graae, B.J., Wallander, H., Fogelberg, E., Wardle, D.A., 2011. Interactive effects of vegetation type and elevation on aboveground and belowground properties in a subarctic tundra. Oikos 120, 128–142. https://doi.org/10.1111/j.1600-0706.2010.18811.x.
Sundqvist, M.K., Sanders, N.J., Dorrepaal, E., Lindén, E., Metcalfe, D.B., Newman, G.S., Olofsson, J., Wardle, D.A., Classen, A.T., 2020. Responses of tundra plant community carbon flux to experimental warming, dominant species removal and elevation. Functional Ecology 1–10. https://doi.org/10.1111/1365-2435.13567.
Sundqvist, M.K., Wardle, D.A., Olofsson, E., Giesler, R., Gundale, M.J., 2012. Chemical properties of plant litter in response to elevation: subarctic vegetation challenges phenolic allocation theories. Functional Ecology 26, 1090–1099. https://doi.org/10.1111/j.1365-2435.2012.02034.x.
Templer, P.H., Mack, M.C., Chapin III, F.S., Christenson, L.M., Compton, J.E., Crook, H. D., Currie, W.S., Curtis, C.J., Dail, D.B., D'Antonio, C.M., Emmett, B.A., Epstein, H. E., Goodale, C.L., Gundersen, P., Hobbie, S.E., Holland, K., Hooper, D.U., Hungate, B. A., Lamontagne, S., Nadelhoffer, K.J., Osenberg, C.W., Perakis, S.S., Schleppi, P., Schimel, J., Schmidt, I.K., Sommerkorn, M., Spoelstra, J., Tietema, A., Wessel, W.W., Zak, D.R., 2012. Sinks for nitrogen inputs in terrestrial ecosystems: a meta-analysis

of 15 N tracer field studies. Ecology 93, 1816–1829. https://doi.org/10.1890/11-1146.1.
Väisänen, M., Sjögersten, S., Large, D., Drage, T., Stark, S., 2015. Long-term Reindeer Grazing Limits Warming-Induced Increases in CO2 Released by Tundra Heath Soil: Potential Role of Soil C Quality. Environmental Research Letters 10. https://doi.org/10.1088/1748-9326/10/9/094020.
Väisänen, M., Ylänne, H., Kaarlejärvi, E., Sjögersten, S., Olofsson, J., Crout, N., Stark, S., 2014. Consequences of warming on tundra carbon balance determined by reindeer grazing history. Nature Climate Change 4, 384–388. https://doi.org/10.1038/nclimate2147.
Vancampenhout, K., Wouters, K., De Vos, B., Buurman, P., Swennen, R., Deckers, J., 2009. Differences in chemical composition of soil organic matter in natural ecosystems from different climatic regions - a pyrolysis-GC/MS study. Soil Biology and Biochemistry 41, 568–579. https://doi.org/10.1016/j.soilbio.2008.12.023.
Veen, G.F., Sundqvist, M.K., Wardle, D.A., 2015. Environmental factors and traits that drive plant litter decomposition do not determine home-field advantage effects. Functional Ecology 29, 981–991. https://doi.org/10.1111/1365-2435.12421.
Walker, D.A., Raynolds, M.K., Daniëls, F.J.A., Einarsson, E., Elvebakk, A., Gould, W.A., Katenin, A.E., Kholod, S.S., Markon, C.J., Melnikov, E.S., Moskalenko, N.G., Talbot, S.S., Yurtsev, B.A., The other members of the CAVM Team, 2005. The Circumpolar Arctic vegetation map. Journal of Vegetation Science 16, 267–282. https://doi.org/10.1111/j.1654-1103.2005.tb02365.x.
Walker, T.W.N., Kaiser, C., Strasser, F., Herbold, C.W., Leblans, N.I.W., Woebken, D., Janssens, I.A., Sigurdsson, B.D., Richter, A., 2018. Microbial temperature sensitivity and biomass change explain soil carbon loss with warming. Nature Climate Change 8, 885–889. https://doi.org/10.1038/s41558-018-0259-x.
Wang, P., Heijmans, M.M.P.D., Mommer, L., van Ruijven, J., Maximov, T.C., Berendse, F., 2016. Belowground Plant Biomass Allocation in Tundra Ecosystems and its Relationship with Temperature. Environmental Research Letters 11. https://doi.org/10.1088/1748-9326/11/5/055003, 055003.
Wardle, D.A., Bardgett, R.D., Klironomos, J.N., Setälä, H., van der Putten, W.H., Wall, D. H., 2004. Ecological linkages between aboveground and belowground biota. Science 304, 1629–1633. https://doi.org/10.1126/science.1094875.
Warren, J.M., Iversen, C.M., Garten, C.T., Norby, R.J., Childs, J., Brice, D., Evans, R.M., Gu, L., Thornton, P., Weston, D.J., 2012. Timing and magnitude of C partitioning through a young loblolly pine (Pinus taeda L.) stand using 13C labeling and shade treatments. Tree Physiology 32, 799–813. https://doi.org/10.1093/treephys/tpr129.
Wookey, P.A., Aerts, R., Bardgett, R.D., Baptist, F., Bråthen, K., Cornelissen, J.H.C., Gough, L., Hartley, I.P., Hopkins, D.W., Lavorel, S., Shaver, G.R., 2009. Ecosystem feedbacks and cascade processes: understanding their role in the responses of Arctic and alpine ecosystems to environmental change. Global Change Biology 15, 1153–1172. https://doi.org/10.1111/j.1365-2486.2008.01801.x.
Xue, K., Yuan, M.M., Shi, Z.J>, Qin, Y., Deng, Y., Cheng, L., Wu, L., He, Z., Van Nostrand, J.D., Bracho, R., Natali, S., Schuur, E.A.G., Luo, C., Konstantinidis, K.T., Wang, Q., Cole, J.R., Tiedje, J.M., Luo, Y., Zhou, J., 2016. Tundra soil carbon is vulnerable to rapid microbial decomposition under climate warming. Nature Climate Change 6, 595–600. https://doi.org/10.1038/nclimate2940.
Yu, Q., Epstein, H., Engstrom, R., Walker, D., 2017. Circumpolar arctic tundra biomass and productivity dynamics in response to projected climate change and herbivory. Global Change Biology 23, 3895–3907. https://doi.org/10.1111/gcb.13632.
Zagal, E., 1994. Influence of light intensity on the distribution of carbon and consequent effects on mineralization of soil nitrogen in a barley (Hordeum vulgare L.)-soil system. Plant and Soil 160, 21–31. https://doi.org/10.1007/BF00150342.
Zak, D.R., Pellitier, P.T., Argiroff, W.A., Castillo, B., James, T.Y., Nave, L.E., Averill, C., Beidler, K.V., Bhatnagar, J., Blesh, J., Classen, A.T., Craig, M., Fernandez, C.W., Gundersen, P., Johansen, R., Koide, R.T., Lilleskov, E.A., Lindahl, B.D., Nadelhoffer, K.J., Phillips, R.P., Tunlid, A., 2019. Exploring the role of ectomycorrhizal fungi in soil carbon dynamics. New Phytologist. https://doi.org/10.1111/nph.15679.
Zelles, L., 1999. Fatty acid patterns of phospholipids and lipopolysaccharides in the characterisation of microbial communities in soil: a review. Biology and Fertility of Soils 29, 111–129. https://doi.org/10.1007/s003740050533.